THE JOURNAL OF BIOLOGICAL CHEMISTRY VOL. 284, NO. 29, pp. 19380–19391, July 17, 2009

Repeated Domains of *Leptospira* Immunoglobulin-like Proteins Interact with Elastin and Tropoelastin*[S]

Received for publication, April 6, 2009, and in revised form, May 15, 2009 Published, JBC Papers in Press, May 27, 2009, DOI 10.1074/jbc.M109.004531

Yi-Pin Lin[‡], Dae-Won Lee[‡], Sean P. McDonough[§], Linda K. Nicholson[¶], Yogendra Sharma[‖], and Yung-Fu Chang[‡1]

From the [‡]Department of Population Medicine and Diagnostic Sciences, [§]Department of Biomedical Science, College of Veterinary Medicine, and [¶]Department of Molecular Biology and Genetics, College of Agriculture and Life Science, Cornell University, Ithaca, New York 14853 and the [‖]Center for Cellular and Molecular Biology, Uppal Road, Hyderabad 500 007, India

***Leptospira* spp., the causative agents of leptospirosis, adhere to components of the extracellular matrix, a pivotal role for colonization of host tissues during infection. Previously, we and others have shown that *Leptospira* immunoglobulin-like proteins (Lig) of *Leptospira* spp. bind to fibronectin, laminin, collagen, and fibrinogen. In this study, we report that *Leptospira* can be immobilized by human tropoelastin (HTE) or elastin from different tissues, including lung, skin, and blood vessels, and that Lig proteins can bind to HTE or elastin. Moreover, both elastin and HTE bind to the same LigB immunoglobulin-like domains, including LigBCon4, LigBCen7′–8, LigBCen9, and LigBCen12 as demonstrated by enzyme-linked immunosorbent assay (ELISA) and competition ELISAs. The LigB immunoglobulin-like domain binds to the 17th to 27th exons of HTE (17–27HTE) as determined by ELISA (LigBCon4, K_D = 0.50 μM; LigBCen7′–8, K_D = 0.82 μM; LigBCen9, K_D = 1.54 μM; and LigBCen12, K_D = 0.73 μM). The interaction of LigBCon4 and 17–27HTE was further confirmed by steady state fluorescence spectroscopy (K_D = 0.49 μM) and ITC (K_D = 0.54 μM). Furthermore, the binding was enthalpy-driven and affected by environmental pH, indicating it is a charge-charge interaction. The binding affinity of LigBCon4D341N to 17–27HTE was 4.6-fold less than that of wild type LigBCon4. In summary, we show that Lig proteins of *Leptospira* spp. interact with elastin and HTE, and we conclude this interaction may contribute to *Leptospira* adhesion to host tissues during infection.**

Pathogenic *Leptospira* spp. are spirochetes that cause leptospirosis, a serious infectious disease of people and animals (1, 2). Weil syndrome, the severe form of leptospiral infection, leads to multiorgan damage, including liver failure (jaundice), renal failure (nephritis), pulmonary hemorrhage, meningitis, abortion, and uveitis (3, 4). Furthermore, this disease is not only prevalent in many developing countries, it is reemerging in the United States (3). Although leptospirosis is a serious worldwide zoonotic disease, the pathogenic mechanisms of *Leptospira* infection remain enigmatic. Recent breakthroughs in applying genetic tools to *Leptospira* may facilitate studies on the molecular pathogenesis of leptospirosis (5–8).

The attachment of pathogenic *Leptospira* spp. to host tissues is critical in the early phase of *Leptospira* infection. *Leptospira* spp. adhere to host tissues to overcome mechanical defense systems at tissue surfaces and to initiate colonization of specific tissues, such as the lung, kidney, and liver. *Leptospira* invade hosts tissues through mucous membranes or injured epidermis, coming in contact with subepithelial tissues. Here, certain bacterial outer surface proteins serve as microbial surface components recognizing adhesive matrix molecules (MSCRAMMs)[2] to mediate the binding of bacteria to different extracellular matrices (ECMs) of host cells (9). Several leptospiral MSCRAMMs have been identified (10–18), and we speculate that more will be identified in the near future.

Lig proteins are distributed on the outer surface of pathogenic *Leptospira*, and the expression of Lig protein is only found in low passage strains (14, 16, 17), probably induced by environmental cues such as osmotic or temperature changes (19). Lig proteins can bind to fibrinogen and a variety of ECMs, including fibronectin (Fn), laminin, and collagen, thereby mediating adhesion to host cells (20–23). Lig proteins also constitute good vaccine candidates (24–26).

Elastin is a component of ECM critical to tissue elasticity and resilience and is abundant in skin, lung, blood vessels, placenta, uterus, and other tissues (27–29). Tropoelastin is the soluble precursor of elastin (28). During the major phase of elastogenesis, multiple tropoelastin molecules associate through coacervation (30–32). Because of the abundance of elastin or tropoelastin on the surface of host cells, several bacterial MSCRAMMs use elastin and/or tropoelastin to mediate adhesion during the infection process (33–35).

Because leptospiral infection is known to cause severe pulmonary hemorrhage (36, 37) and abortion (38), we hypothesize that some leptospiral MSCRAMMs may interact with elastin and/or tropoelastin in these elastin-rich tissues. This is the first report that Lig proteins of *Leptospira* interact with

* This work was supported in part by the Harry M. Zweig Memorial Fund for Equine Research, the New York State Science and Technology Foundation (Center for Advanced Technology), and the Biotechnology Research and Development Corp.

[S] The on-line version of this article (available at http://www.jbc.org) contains supplemental Figs. 1 and 2.

[1] To whom correspondence should be addressed: Dept. of Population Medicine and Diagnostic Sciences, College of Veterinary Medicine, Cornell University, Ithaca, NY 14853. Tel.: 607-253-2675; Fax: 607-253-3943; E-mail: yc42@cornell.edu.

[2] The abbreviations used are: MSCRAMM, microbial surface components recognizing adhesive matrix molecules; HTE, human tropoelastin; Fn, fibronectin; ITC, isothermal titration calorimetry; ELISA, enzyme-linked immunosorbent assay; Lig, *Leptospira* immunoglobulin-like; BSA, bovine serum albumin; HRP, horseradish peroxidase; GST, glutathione *S*-transferase; ECM, extracellular matrix.

elastin and tropoelastin, and the interactions are mediated by several specific immunoglobulin-like domains of Lig proteins, including LigBCon4, LigBCen7′–8, LigBCen9, and LigBCen12, which bind to the 17th to 27th exons of human tropoelastin (HTE).

MATERIALS AND METHODS

Bacterial Strains—Leptospira interrogans serovar Pomona (NVSL1427-35-093002) was used in this study (18). All experiments were performed with virulent, low passage strains obtained by infecting golden Syrian hamsters as described previously (24). Leptospires were grown in EMJH medium at 30 °C for less than five passages; growth was monitored by dark field microscopy.

Reagents and Antibodies—Rabbit anti-GST antibody and Alexa488-conjugated goat anti-hamster antibody were ordered from Molecular Probes (Eugene, OR). Horseradish peroxidase (HRP)-conjugated goat anti-hamster antibody, HRP-conjugated goat anti-horse antibody, HRP-conjugated goat anti-rabbit antibody, and HRP-conjugated streptavidin were ordered from Kirkegaard & Perry Laboratories (Gaithersburg, MD). Human lung, aortic and skin elastins, and bovine serum albumin (BSA) were ordered from Sigma. The QuikChange mutagenesis kit was purchased from Stratagene (La Jolla, CA). Elastin peptide was ordered from Elastin Products Co. (Owensville, MO). Hamster anti-*L. interrogans* antibodies were previously prepared in hamsters from the challenge controls (24).

Plasmid Construction and Protein Purification—N2-N3 domain of FnBPA (rFnBPA-(194–511)) gene from *Staphylococcus aureus* (34, 39) and the full-length HTE gene (40) were cloned into pQE30 and pTrcHis-TOPO vectors, respectively, and purified as histidine tag fusion proteins. Construction for expression as histidine tag, GST, or maltose-binding protein fused with truncated HTE, including 1–18 HTE (1st to 18th exons of HTE), 17–27 HTE (17th to 27th exons of HTE), and 27–36 HTE (27th to 36th exons of HTE), is shown as a scheme in Fig. 5*A*. Truncated LigB constructs, including LigBCon (amino acids 47–630 in LigB), LigAVar (amino acids 631–1225 in LigA), LigBCen (amino acids 631–1417 in LigB), LigBCtv (amino acids 1418–1889 in LigB), LigBCen1 (amino acids 631–1013 in LigB), LigBCen2 (amino acids 1014–1165 in LigB), LigBCen3 (amino acids 1166–1417 in LigB), LigBCon1–3 (amino acids 47–316 in LigB), LigBCon4–7′ (amino acids 307–630 in LigB), LigBCon4 (amino acids 307–403 in LigB), LigBCon5 (amino acids 397–492 in LigB), LigBCon6–7′ (amino acids 486–630 in LigB), LigB7′–8 (amino acids 631–756 in LigB), LigB9 (amino acids 755–850 in LigB), LigB10 (amino acids 846–941 in LigB), LigB11 (amino acids 942–1028 in LigB), LigB12 (amino acids 1047–1119 in LigB), and LigBCen2NR (amino acids 1120–1165 in LigB) is shown as a scheme in Fig. 2. Each PCR-amplified fragment was inserted into vectors pET-THGT, pET-THMT, pQE30 (Qiagen, Alencia, CA), and/or pGEX-4T-2 (GE Healthcare) as described previously (21, 22, 26). Constructs for the expression of histidine tag or GST-fused LigBCon, LigAVar, LigBCen, LigBCtv, LigBCen1, LigBCen2, LigBCen3, LigBCen2NR, and GST were obtained from previous studies (21, 22, 26, 41) (Fig. 1). Other constructs, including 1–18HTE, 17–27HTE, 27–36HTE, LigBCon1–3, LigBCon4–7, LigBCon4, LigBCon5, LigBCon6–7′, LigB7′–8, LigB9, LigB10, LigB11, and LigB12, were amplified by PCR using the primers described in Table 1 and are based on the DNA sequences derived from GenBank™ (*L. interrogans* serovar Pomona, FJ030916) and human tropoelastin (42). For constructing LigBCon1–3 and LigBCon4–7′, primers were engineered to introduce a SalI site at the 5′ end and a stop codon followed by a NotI site at the 3′ end of each fragment. For LigBCon4, LigBCon5, LigBCon6, LigBCen7′–8, LigB9, LigB10, LigB11, and LigB12 fragments, primers were engineered to introduce an SphI site at the 5′ end and a stop codon followed by a SalI site at the 3′ end of each fragment (Table 1). PCR products were sequentially digested with either SalI and NotI or SphI and SalI and inserted into pQE30 or pGEX-4T-2 cut with appropriate matching restriction enzyme sets. Sets of primers were engineered to introduce an EcoRI site at the 5′ end and a stop codon followed by a NotI site at the 3′ end of each fragment in constructing 1–18HTE, 17–27HTE, and 27–36HTE clones (Table 1). PCR products were sequentially digested with EcoRI and NotI and then ligated into pET-THMT or pET-THGT (obtained from the Cornell Protein Production and Characterization Core Facility, Cornell University) cut with EcoRI and NotI, respectively. For LigBCon4D35N mutant construction, the pQE30 expression plasmid containing the DNA sequence encoding LigBCon4 was subjected to site-directed mutagenesis using the QuikChange mutagenesis kit following the manufacturer's instructions (Stratagene, La Jolla, CA). Resulting PCR products were digested with DpnI to remove contaminating wild type plasmid and then transformed into *Escherichia coli*

TABLE 1
Primers

Primer/Vector	Sequence[a]
LigBCon1–3fp/pGEX4T2[b]	CGGTCGACTGGTAACTCTAATCCG
LigBCon1–3rp	CGGCGGCCGCAATAGAAACTAAGGC
LigBCon4–7′fp/pGEX4T2	CGGTCGACTATCGTTACTCCAGCA
LigBCon4–7′rp	CGGCGGCCGCAATATCCGTATTAGA
LigBCon4fp/pQE30[c]	CGGCATGCATCGTTACTCCAGCA
LigBCon4rp	CGGTCGACTAATACCTCTTGTGT
LigBCon5fp/pQE30	CGGCATGCAAAGTTACACAAGAG
LigBCon5rp	CGGTCGACGAGAACCGCAGGAAC
LigBCon6–7′fp/pQE30	CGGCATGCACTGTAGTTCCTGCG
LigBCon6–7′rp	CGGTCGACAATATCCGTATTAGA
LigBCen7′–8fp/pQE30	CGCGGATCCATTGCTGAAATT
LigBCen7′–8rp	CGCCCTGCAGGACATTCAAAAC
LigBCen9fp/pQE30	CGGCATGCAATGTCACTCCTGCA
LigBCen9rp	CGGTCGACTAAGTCAGTGACTGT
LigBCen10fp/pQE30	CGGCATGCACAGTCACTGACTTA
LigBCen10rp	CGGTCGACGGCAGCACTTACATT
LigBCen11fp/pQE30	CGGGATCCACGTTAGATTCCATT
LigBCen11rp	CGAAGCTTTTAGACCGTTATGTC
LigBCen12fp/pQE30	CGGGATCCACCCTTTCTTCGATT
LigBCen12rp	CGAAGCTTTTATACTGTGAGAATTGT
LigBCon4D341N[d]	GGGATCTTTACAAATAATTCAAACTCG
LigBCon4D341Nr[d]	CGAGTTTGAATTATTTGTAAAGATCCC
1–18HTEfp/pET-THGT[e]	CGGAATTCATGGCGGGTCTGACGGCG
1–18HTErp	CGGCGGCCGCTGGAACCGCAGCACC
17–27HTEfp/pET-THGT	CGGAATTCGGCGTTGGGACTCCA
17–27HTErp	CGGCGGCCGCTCCATATTTGGCTGC
27–36HTEfp/pET-THMT[e]	CGGAATTCGTACCTGGAGCCCTG
27–36HTErp	CGGCGGCCGCTTTTCTCTTCCGGCC

[a] The restriction enzyme cutting sites are underlined.
[b] Plasmid was obtained from GE Healthcare.
[c] Plasmid was obtained from Qiagen Inc., Valencia, CA.
[d] Primed were used for site-directed mutagenesis.
[e] Plasmids were obtained from the Cornell Protein Production and Characterization Core Facility, Cornell University.

XL-1 Blue (Stratagene, La Jolla, CA). Transformants were screened and subjected to DNA sequencing. In this study, we purified the soluble form of the histidine tag, GST, or maltose-binding fusion proteins from *E. coli* as described previously (21, 23, 41).

Bacterial Adhesion to Immobilized Elastin or Tropoelastin Measured by ELISA and Epifluorescence Microscope—To measure the binding of *Leptospira* to elastin or tropoelastin, 100 μl of 10 μg/ml human lung elastin, chicken tropoelastin, or BSA (negative control) were coated onto microtiter plate wells. For dose-dependent binding experiments, 100 μl of different concentrations of each human lung, aortic and skin elastins, chicken tropoelastin, or BSA were coated onto microtiter plate wells. To immobilize elastin, all of the elastins were dissolved in coating buffer (0.1 M sodium bicarbonate, pH 9.4) and then air-dried under UV light (355 nm) at room temperature for 18 h as described previously (35). To immobilize tropoelastin or BSA, tropoelastin or BSA was dissolved in Tris buffer (25 mM Tris and 150 mM sodium chloride, pH 7.5), added to microtiter plate wells, and incubated at 4 °C overnight (21, 22, 43). After the plates were subsequently blocked with blocking buffer (100 μl/well) containing 3% BSA in Tris buffer at room temperature for 2 h, *Leptospira* (10^7) were added to each well and further incubated at 37 °C for 6 h. Following incubation, the plates were washed three times with Tris buffer containing 0.05% Tween 20 (TBST). To measure the binding of *Leptospira*, hamster anti-*Leptospira* (1:200) and HRP-conjugated goat anti-hamster IgG (1:1000) were used as primary and secondary antibodies, respectively. After washing the plates three times with TBST, 100 μl of 3,3′,5,5′-tetramethylbenzidine (Kirkegaard & Perry Laboratories) were added to each well and incubated for 5 min. The reaction was stopped by adding 100 μl of 0.5% hydrofluoric acid to each well. Each plate was read at 630 nm by an ELISA plate reader (Biotek EL-312, Winooski, VT). Each value represents the mean ± S.E. of three trials in triplicate samples. Statistically significant ($p < 0.05$) differences are indicated by an asterisk.

To measure the binding of *Leptospira* to elastin or tropoelastin by epifluorescence microscopy, *Leptospira* (10^8) were added to each well (eight well culture slides) coated with 1 μg of human lung elastin, chicken tropoelastin, or BSA (negative control) in 100 μl of Tris buffer and incubated at 37 °C for 6 h. For the detection of *Leptospira* binding in Fig. 2*B*, hamster anti-*Leptospira* antibodies (1:100) and Alexa 488-conjugated goat anti-hamster IgG (1:250) were used as primary and secondary antibodies, respectively. Fixation and immunofluorescence staining were performed as described previously (22) with slight modifications. Briefly, *Leptospira* were fixed in 2% paraformaldehyde for 60 min at room temperature. For antibody labeling, fixed bacteria were incubated in Tris buffer containing 0.3% BSA for 10 min at room temperature. The primary and secondary antibodies, diluted in Tris buffer containing 0.3% BSA, were incubated sequentially for 60 min at room temperature. After incubation with the primary and secondary antibodies, the glass slides were mounted with coverslips using Prolong Antifade (Molecular Probe) and viewed with a ×60 objective by epifluorescence microscope (Nikon, Japan). The settings were identical for all captured images. Images were processed using Adobe Photoshop CS2.

Elastin and Tropoelastin Binding Assays—100 μl of 10 μg/ml human lung elastin, HTE, or BSA (negative control and data not shown) was coated onto microtiter plate wells as described above. 100 μl of different concentrations of biotinylated LigBCon, LigAVar, LigBCen, LigBCtv, LigBCon1–3, LigBCon4–7′, LigBCen1, LigBCen2, LigBCen3, LigBCon4, LigBCon5, LigBCon6–7′, LigBCen7′–8, LigBCen9, LigBCen10, LigBCen11, LigBCen12, LigBCen2NR, or rFnBPA-(194–511) (positive control), or biotin (negative control) were added subsequently (Fig. 3). To reveal the HTE-binding sites of Lig protein, 100 μl of 1 μM full-length HTE and truncated HTE, including 1–18HTE, 17–27HTE, 27–36HTE, or BSA (negative control), were coated onto microtiter plate wells, and 100 μl of different concentrations of biotinylated LigBCon4, LigBCen7′–8, LigBCen9, LigBCen12, or biotin (negative control) were added subsequently (Fig. 5). To detect binding of biotinylated proteins, HRP-conjugated streptavidin (1:1000) was added to each well at room temperature for 1 h prior to washing the wells three times with TBST. The measurement of binding by ELISA was as described above. To determine the dissociation constant (K_D), the data were fitted as shown in Equation 1 by using KaleidaGraph software (version 2.1.3 Abelbeck software, Reading, PA), and the calculated K_D values are listed in Table 2.

$$OD_{630} = \frac{OD_{630max}[\text{Lig proteins}]}{K_D + [\text{Lig proteins}]} \quad \text{(Eq. 1)}$$

Inhibition of LigBCon4, LigBCen7′–8, LigBCen9, LigBCen12, and rAFnBPA-(194–511) Binding to Immobilized Elastin or Tropoelastin with Soluble Elastin Peptides or Tropoelastin—The wells of a microtiter plate were coated with 100 μl of 10 μg/ml human lung elastin, HTE, or BSA (negative control) as described previously. 100 μl of 1 μM biotinylated LigBCon4, LigBCen7′–8, LigBCen9, LigBCen12, rAFnBPA-(194–511) (positive control), or biotin (negative control) were mixed with different concentrations of soluble lung elastin peptides or HTE at room temperature for 1 h prior to be added to elastin or HTE-coated wells (Fig. 4). The binding of biotinylated proteins was measured by ELISA as described above.

Steady State Fluorescence Measurement—Steady state fluorescence emissions were measured on a Hitachi F4500 spectrofluorometer (Hitachi. San Jose, CA). All spectra were recorded in correct spectrum mode of the instrument using excitation and emission band passes of 2 nm. The intrinsic tryptophan fluorescence of 1 μM wild type LigBCon4 or LigBCon4D35N was recorded by exciting the solution at 295 nm and measuring the emission in the 305–400-nm regions. For truncated tropoelastin titration, 0.4, 0.8, 1.6, 3.2, 6.4, or 12.8 μM 1–18HTE, 17–27HTE, 27–36HTE in Tris buffer (25 mM Tris, 150 mM sodium chloride, pH 7.5) was mixed with 1 μM LigBCon4 or LigBCon4D35N. For measuring the pH effect on LigBCon4 (1 μM) binding to 17–27HTE, the same serial dilutions of 17–27HTE mentioned above using Tris buffer with pH ranging from 4.5 to 9.5, as described in Fig.

TABLE 2
The dissociation constant (K_D) obtained from the Elastin and HTE binding by Lig proteins determined by ELISA

Truncated Lig	K_D				
	Elastin	HTE	1–18HTE	17–27HTE	27–36HTE
LigBCon	166 ± 38 nM	ND[a]	ND[a]	ND[a]	ND[a]
LigBCon1–3	NB[b]	ND[a]	ND[a]	ND[a]	ND[a]
LigBCon4–7	181 ± 33 nM	ND[a]	ND[a]	ND[a]	ND[a]
LigBCon4	179 ± 29 nM	475 ± 80 nM	NB[b]	501 ± 51 nM	NB[b]
LigBCon5	NB[b]	ND[a]	ND[a]	ND[a]	ND[a]
LigBCon6–7′	NB[b]	ND[a]	ND[a]	ND[a]	ND[a]
LigAVar	NB[b]	ND[a]	ND[a]	ND[a]	ND[a]
LigBCen	101 ± 11 nM	ND[a]	ND[a]	ND[a]	ND[a]
LigBCen1	189 ± 21 nM	ND[a]	ND[a]	ND[a]	ND[a]
LigBCen7′–8	750 ± 56 nM	824 ± 17 nM	NB[b]	833 ± 13 nM	NB[b]
LigBCen9	1230 ± 15 nM	1390 ± 11 nM	NB[b]	1540 ± 351 nM	NB[b]
LigBCen10	NB[b]	ND[a]	ND[a]	ND[a]	ND[a]
LigBCen11	NB[b]	ND[a]	ND[a]	ND[a]	ND[a]
LigBCen12	208 ± 25 nM	726 ± 20 nM	NB[b]	742 ± 31 nM	NB[b]
LigBCen2	212 ± 34 nM	ND[a]	ND[a]	ND[a]	ND[a]
LigBCen2NR	NB[b]	ND[a]	ND[a]	ND[a]	ND[a]
LigBCen3	NB[b]	ND[a]	ND[a]	ND[a]	ND[a]
LigBCtv	NB[b]	ND[a]	ND[a]	ND[a]	ND[a]
$rFnBPA_{194–511}$	42 ± 1.5 nM	133 ± 22 nM	ND[a]	ND[a]	ND[a]

[a] ND indicates not determined.
[b] NB indicates no binding.

TABLE 3
Thermodynamic parameters for the interaction of 17–27HTE and LigBCon4 or LigBCon4D341N

	[Proteins]	[HTE]	ΔH	$T\Delta S$	K_D	ΔG	n
	μM	μM	kcal mol^{-1}	kcal mol^{-1} K^{-1}	μM	kcal mol^{-1}	
LigBCon4	20	1	−46.39	−37.88	0.54 ± 0.02	−8.51	1.01
LigBCon4D341N	20	1	−56.68	−49.05	2.51 ± 0.48	−7.63	0.99

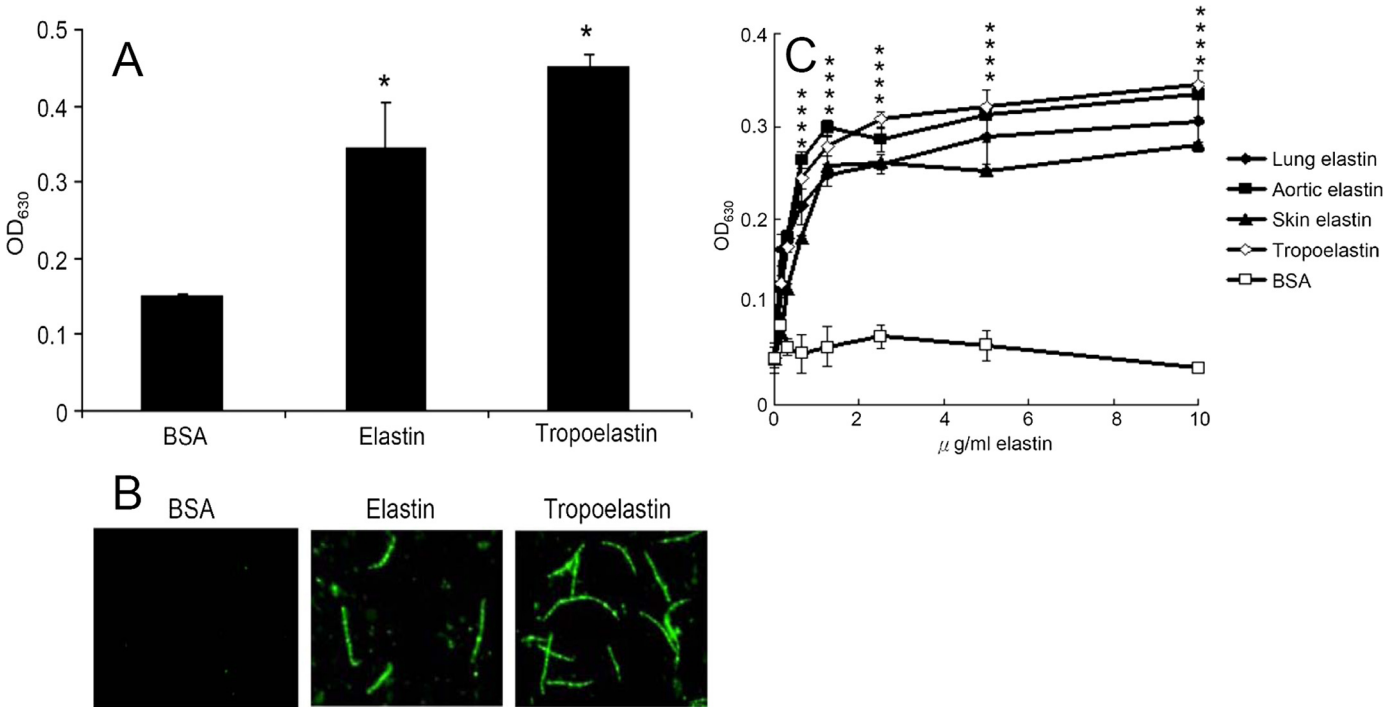

FIGURE 1. **Binding of *L. interrogans* serovar Pomona (NVSL 1427-35-093002) to elastin and tropoelastin.** *A,* binding of *Leptospira* to BSA, elastin, or tropoelastin. *Leptospira* (10^7) were added to wells coated with BSA, human lung elastin, or HTE (1 μg in 100 μl of Tris buffer). *B,* binding of *Leptospira* to immobilized elastin or HTE. *Leptospira* (10^8) were cultured in human lung elastin-, THE-, or BSA-coated (negative control) (1 μg in 100 Tris buffer) or -uncoated wells (negative control). Leptospiral immobilization was assayed by immunofluorescence microscopy. *C,* binding of *Leptospira* (10^7) to various concentrations of human lung elastin, human aortic elastin, human skin elastin, HTE, or BSA (0, 0.25, 0.5, 1, 2, 4, 8, and 16 μg/ml in 100 μl of Tris buffer). BSA serves as negative control. *A* and *C,* the binding of *Leptospira* was estimated by ELISA, and each value represents the mean ± S.E. of three trials performed in triplicate samples. Statistically significant ($p < 0.05$) differences compared with the negative reference are indicated by an *asterisk*.

7*C,* were used. All spectra were recorded at 25 °C after 5 min. Furthermore, the spectra of the various concentrations of HTE indicated above were also recorded and used to subtract the spectra of each Lig protein in the addition of certain concentrations of HTE. To determine the dissociation constant (K_D), the fluorescence intensities at 320 nm were

recorded and fitted as shown in Equation 2 using KaleidaGraph software (version 2.1.3 Abelbeck software),

$$F_{max} - F = \frac{(F_{max} - F_{min})[\text{tropoelastin}]}{K_D + [\text{tropoelastin}]} \quad \text{(Eq. 2)}$$

where F_{max} is the fluorescence intensity of Lig proteins in the absence of HTE; F_{min} indicates the fluorescence intensities of Lig proteins saturated with HTE. In addition, F is the fluorescence intensities of Lig proteins in the presence of various concentrations of HTE. All of the measurements were corrected for dilution and for inner filter effect.

Calculation of Charges on LigBCon4 and 17–27HTE at Different pH Values—The charges on LigBCon4 at different pH values and 17–27HTE were determined using ABIM, a web service for remote and automatic data processing. The analyses were performed using default values.

Isothermal Titration Calorimetry (ITC)—The experiments were carried out with a CSC 5300 microcalorimeter (Calorimetry Science Corp., Lindon, UT) at 25 °C as described previously (21, 22). In a typical experiment, the cell contained 1 ml of a solution of LigBCon4 or LigBCon4D35N, and the syringe contained 250 μl of a solution of 17–27HTE. The concentration of Lig proteins and 17–27HTE are detailed in Table 3. Both solutions were in Tris buffer, pH 7.5. The titration was performed as follows: 25 injections of 10 μl with a stirring speed of 250 rpm with a delay time between injections of 5 min. Data were analyzed using Titration Binding Work 3.1 software (Calorimetry Science Corp.) fitting them to an independent binding model.

CD Spectroscopy—CD analysis was performed on an Aviv 215 spectropolarimeter (Lakewood, NJ) under N_2 atmosphere. CD spectra were measured at room temperature (25 °C) in a 1-cm path length quartz cell. Spectra of LigBCon4 and LigBCon4D35N were recorded in Tris buffer, pH 7.5, at a protein concentration of 10 μM. Three spectra were recorded for each condition from 190 to 250 nm for far-UV CD in 1-nm increments. To reveal the effect of pH, 10 μM LigBCon4 or 17–27HTE in Tris buffer ranging from pH 4.5 to 9.5 was used in all CD experiments. The background spectrum of buffer without protein was subtracted from the protein spectra. CD spectra were initially analyzed by the software accompanying the spectrophotometer. Analysis of spectra to extrapolate secondary structures was performed by Dichroweb (44) using the K2D and Selcon 3 analysis programs (45, 46).

Statistical Analysis—Significant differences between samples were determined using the Student's t test following logarithmic transformation of the data. Two-tailed p values were determined for each sample, and a p value <0.05 was considered significant. Each data point represents the mean ± S.E. for each sample tested in triplicate. An asterisk indicates the result was statistically significant.

RESULTS

Leptospira Can Be Immobilized by Elastin and Tropoelastin—To determine whether leptospiral adherence is mediated by elastin, ELISA-based and immunofluorescence assays were performed. As shown on Fig. 1, *A* and *B*, both elastin and its precursor, tropoelastin, can immobilize *Leptospira* on microtiter plate wells or culture slides.

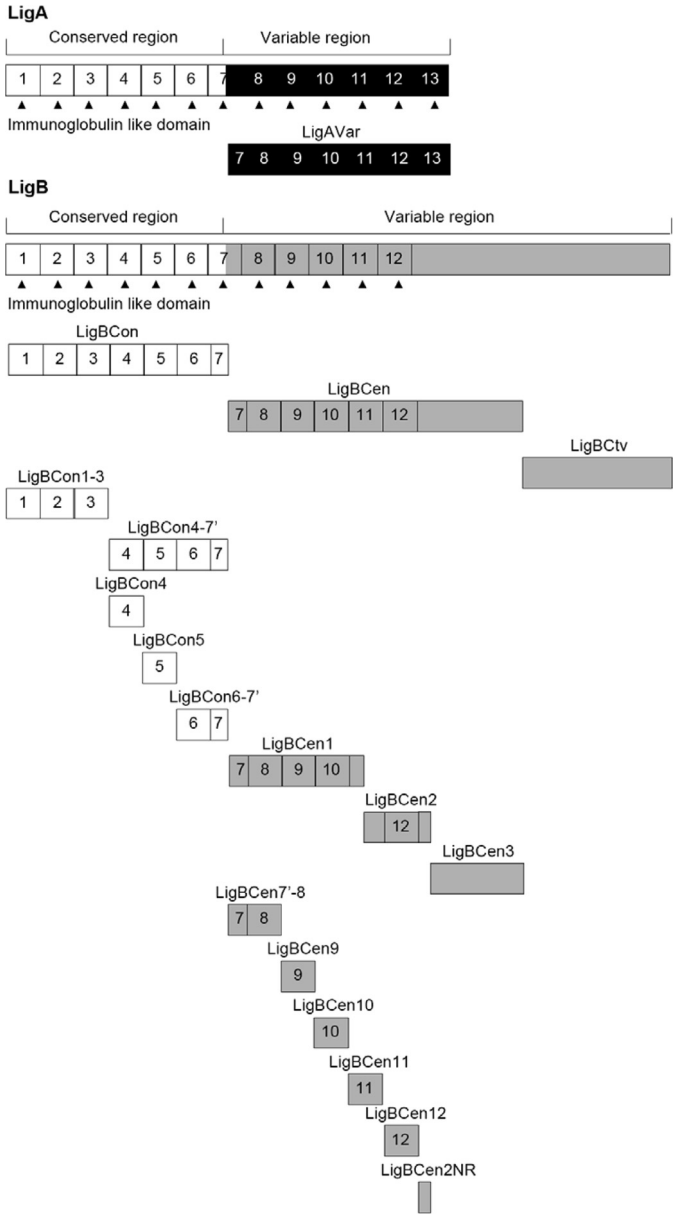

FIGURE 2. **A schematic diagram showing the structure of Lig proteins and the truncated Lig proteins used in this study.**

To reveal whether elastin derived from different tissues affects the immobilization of *Leptospira*, *Leptospira* were incubated over various concentrations of human lung, aortic or skin elastin coated onto microtiter plate wells. Based on the results of Fig. 1*C*, *Leptospira* can bind to elastin from all different sources, including lung, skin, and blood vessels.

LigBCon4, LigBCen7′–8, LigBCen9, and LigBCen12 Mediate the Binding of Leptospira to Elastin and Tropoelastin—To examine LigA- and LigB-mediated leptospiral adhesion to elastin, Lig proteins were truncated and expressed as shown in Fig. 2. First, biotinylated LigBCon, LigAVar, LigBCen, LigBCtv, or biotin (negative control) was added to elastin-coated microtiter plate wells. In addition, rFnBPA-(194–511) was used as a positive control (33, 35). As indicated in Fig. 3*A*, only LigBCon and LigBCen can bind to elastin (LigBCon, K_D = 166 ± 38 nM; LigBCen, K_D = 101 ± 11 nM). To further localize the elastin-

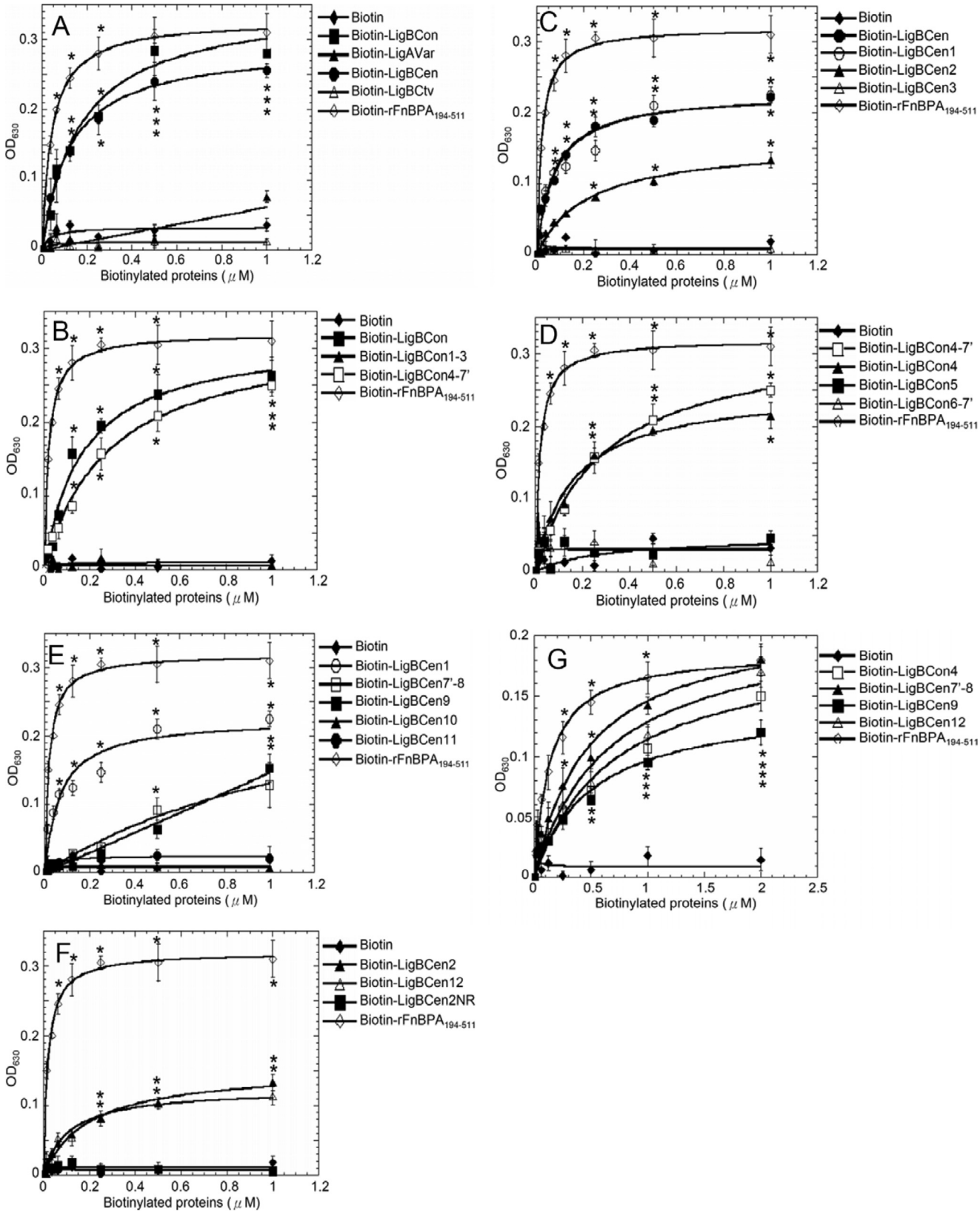

FIGURE 3. **Localization of the elastin or HTE binding domains on Lig proteins.** Various concentrations (0.0156, 0.03125, 0.0625, 0.125, 0.25, 0.5, and 1 μM) of biotin (negative control), biotinylated rAFnBPA-(194–511) are as follows: *A*, LigBCon, LigAVar, LigBCen, and LigBCtv; *B*, LigBCon, LigBCon1–3, and LigBCon4–7′; *C*, LigBCen, LigBCen1, LigBCen2, and LigBCen3; *D*, LigBCon4′-7, LigBCon4, LigBCon5, and LigBCon6–7′; *E*, LigBCen1, LigBCen7′–8, LigBCen9, LigBCen10, and LigBCen11; *F*, LigBCen2, LigBCen12, or LigBCen2NR; and *G*, LigBCon4, LigBCen7′–8, LigBCen9, and LigBCen12 were added to wells coated with 1 μg of BSA (negative control and data not shown). *A–F*, human lung elastin; *G*, HTE in Tris buffer. The binding of biotinylated proteins to elastin or HTE was measured by ELISA. For all experiments, each value represents the mean ± S.E. of three trials in triplicate samples. Statistically significant ($p < 0.05$) differences compared with negative control are indicated by an *asterisk*.

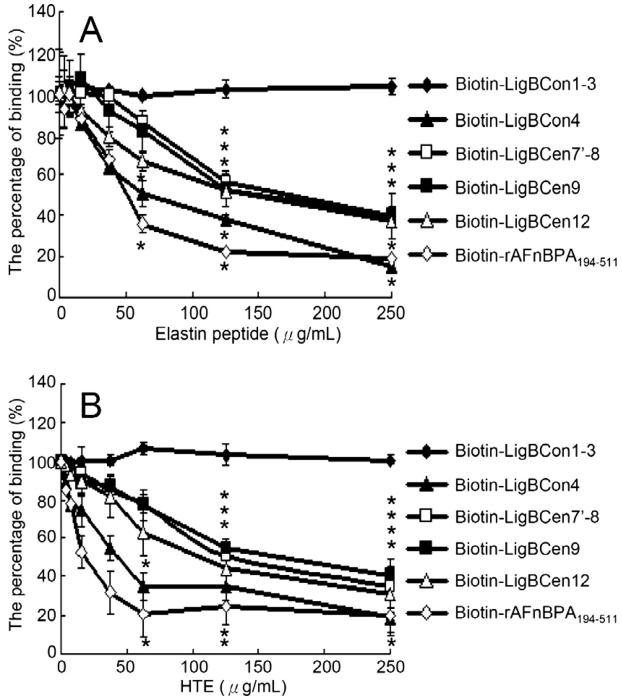

FIGURE 4. **Soluble elastin peptide or HTE inhibited LigBCon4, LigBCen7′-8, LigBCen9, LigBCen12 binding to immobilized elastin or HTE.** One μM of LigBCon1–3 (negative control), biotinylated rAFnBPA-(194–511) (positive control) LigBCon4, LigBCen7′–8, LigBCen9, and LigBCen12 treated with various concentrations (3.90, 7.81, 15.62, 31.25, 62.5, 125, and 250 μg/ml in 100 μl of Tris buffer) of soluble elastin peptide or HTE were added to each well coated with 1 μg of BSA (negative control and data not shown). *A,* human lung elastin; *B,* HTE in Tris buffer. The binding of biotinylated proteins to wells was measured by ELISA. The percentage of binding was determined relative to the binding of biotinylated proteins in the untreated well. For all experiments, each value represents the mean ± S.E. of three trials in triplicate samples. Statistically significant ($p < 0.05$) differences compared with the negative reference are indicated by an *asterisk*.

binding sites on LigBCon or LigBCen, truncated LigBCon and LigBCen were constructed, expressed, purified, and biotinylated (Fig. 2), and ELISAs were performed to map the elastin-binding sites. As shown in Fig. 3, *B* and *D*, the elastin-binding site on LigBCon was determined as LigBCon4, the fourth immunoglobulin repeated region of LigBCon (LigBCon4, K_D = 179 ± 29 nM). On the other hand, unlike LigBCon, there were three elastin-binding sites on LigBCen, including LigBCen7′–8, LigBCen9 and LigBCen12 (LigBCen7′–8, K_D = 750 ± 56 nM; LigBCen9, K_D = 1230 ± 15 nM; and LigBCen12, K_D = 208 ± 25 nM) (Fig. 3, *C*, *E,* and *F*).

To investigate whether tropoelastin also binds to similar Lig protein-binding sites as elastin, biotinylated LigBCon4, LigBCen7′–8, LigBCen9, or LigBCen12 was added to HTE-coated microtiter plate wells in a binding assay. As presented in Fig. 3*G*, all four of these regions can also bind to HTE (LigBCon4, K_D = 475 ± 80 nM; LigBCen7′–8, K_D = 824 ± 17 nM; LigBCen9, K_D = 1390 ± 11 nM; and LigBCen12, K_D = 726 ± 20 nM).

Soluble Elastin or HTE Block LigBCon4, LigBCen7′–8, LigBCen9, and LigBCen12 Binding to Elastin or HTE—To further confirm the association of specific Lig domains with elastin or HTE, biotin (negative control) and biotinylated LigBCon4, LigBCen7′–8, LigBCen9, or LigBCen12 was incubated in the presence of soluble elastin or HTE prior to the addition of elastin or HTE-coated microtiter plate wells. As shown in Fig. 4*A*, soluble elastin peptide blocked the interaction of LigBCon4, LigBCen7′–8, LigBCen9, and LigBCen12 with elastin. Pretreatment of these four fragments with HTE also inhibited binding (Fig. 4*B*), suggesting that these fragments contain both THE- and elastin-binding sites.

LigBCon4, LigBCen7′–8, LigBCen9, and LigBCen12 Bind to 17th to 27th Exons of HTE—To locate the binding domain on HTE, biotin (negative control), biotinylated LigBCon4, LigBCen7′–8, LigBCen9, or LigBCen12 was incubated with either full-length HTE or different truncated fragments of THE, including 1–18HTE (1st to 18th exons of HTE), 17–27HTE (17th to 27th exons of HTE), and 27–36HTE (27th to 36th exons of HTE) (Fig. 5*A*) and assayed for their binding activity using ELISA. As indicated in Fig. 5, all four Lig protein fragments only bind to 17–27HTE (LigBCon4, K_D = 0.50 ± 0.051 μM; LigBCen7′–8, K_D = 0.83 ± 0.13 μM; LigBCen9, K_D = 1.54 ± 0.35 μM; and LigBCen12, K_D = 0.74 ± 0.031 μM).

Because the binding affinity of LigBCon4 to 17–27HTE is highest, further studies using steady state fluorescence spectrometry and ITC were used; the results confirm those from the ELISA tests. We found that the tryptophan fluorescence intensity of LigBCon4 in the presence of 17–27HTE (compared with 1–17HTE or 27–36HTE) was quenched; this is in agreement with our ELISA results, indicating that LigBCon4 binds to 17–27HTE (Fig. 6, *A* and *B*). The K_D value obtained from the quenched fluorescence spectra (K_D = 0.49 ± 0.07 μM) matched the data obtained with ELISA very closely (Fig. 6*B*). Furthermore, K_D values from ITC measurements confirmed the binding nature of LigBCon4 to 17–27HTE (K_D = 0.54 ± 0.02 μM) (Fig. 6*C* and Table 3). On the other hand, the negative values of both enthalpy and entropy shown on Table 2 indicated that the binding of LigBCon4 to 17–27HTE was an enthalpy-favorable and entropy-unfavorable interaction. The binding was only driven by enthalpy through charge-charge interactions or van der Waal forces, *i.e.* the surface charges of interface of LigBCon4-17-27HTE might contribute to the binding.

Effect of pH on the LigBCon4-17-27HTE Interaction—Because of the possibility of surface charges for the binding of LigBCon4 to 17–27HTE (Table 3), we further investigated the influence of pH on the interaction of both proteins. An ABIM software program was used to analyze the titration curve of LigBCon4 and 17–27HTE. As shown in Fig. 7*A*, 17–27HTE undergoes a sharp isoelectric transition at pH 9.5 and maintains a positive charge up to pH 9.5. However, there are two steps of transitions from the titration curve of LigBCon4 located around pH 4 and pH 11, and the surface charge of LigBCon4 is kept slightly negative from pH 4 to pH 10 (Fig. 7*A*). The effect of pH on the LigBCon4-17-27HTE interaction was also measured by the quenching of fluorescence intensity of LigBCon4 in the presence of various concentrations of 17–27HTE. As presented in Fig. 7, *B* and *C*, the highest affinity was found in the range of pH 6.5–7.5 (pH 6.5, K_D = 0.60 ± 0.08 μM; pH 7.5, K_D = 0.49 ± 0.07 μM). When pH was lower than 6.5 or higher than 7.5, the binding affinity of LigBCon4-17-27HTE was considerably lower (pH 4.5, K_D = 4.84 ± 0.20 μM; pH 5.5, K_D = 2.53 ± 0.27 μM; pH 8.5, K_D = 2.30 ± 0.20 μM) (Fig. 7*B*);

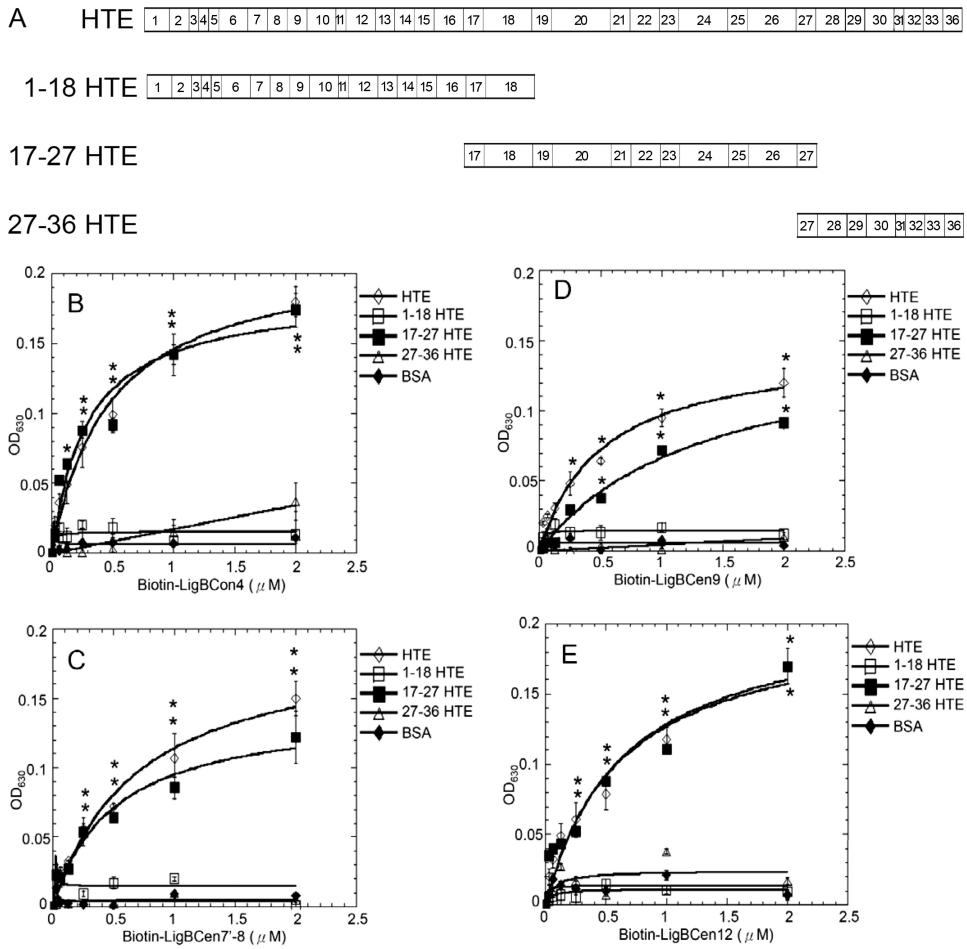

FIGURE 5. **Mapping the binding site of LigBCon4, LigBCen7′-8, LigBCen9, and LigBCen12 on HTE.** *A, chart* presenting the location of HTE and truncated HTE used in this study. *B–E,* binding of LigBCon4, LigBCen7′–8, LigBCen9, and LigBCen12 to various concentrations of immobilized truncated HTE. Various concentrations (0.03125, 0.0625, 0.125, 0.25, 0.5, 1, and 2 μM) of biotin (negative control and data not shown), biotinylated (*B*) LigBCon4, (*C*) LigBCen7′–8, (*D*) LigBCen9, or (*E*) LigBCen12 were added to 1 μM of full-length HTE, 1–18HTE, 17–27HTE, 27–36HTE, or BSA (negative control) in 100 μl of phosphate-buffered saline-coated microtiter plate wells. Bound proteins were measured by ELISA. For all experiments, each value represents the mean ± S.E. of three trials in triplicate samples. Statistically significant ($p < 0.05$) differences compared with the negative control are indicated by an *asterisk*.

interaction was found to be negligible at pH 9.5 or higher (data not shown).

To determine whether the observed reduced affinity was because of conformational changes by LigBCon4 and 17–27HTE when the pH was outside the 6.5–7.5 range, we performed a CD analysis. Results from our undifferentiated CD spectra recorded from pH 4.5 to 9.5 indicate that the reduced affinity was not the result of disruption of the structure of LigBCon4 and 17–27HTE (supplemental Fig. 1). Furthermore, the secondary structures of LigBCon4 and 17–27HTE were shown to be unaffected by various pH environments (supplemental Fig. 1). This indicates that the interaction of LigBCon4 and 17–27HTE is largely influenced by charge-charge interaction via the environmental pH.

Asp-341 Is Critical for the Association of LigBCon4 and 17–27HTE—The results of surface charge prediction showed that the negatively charged amino acids of LigBCon4 at physiological pH might contribute to the interaction of Lig/HTE by charge-charge interaction (Fig. 7*A*). The sequence alignment was performed on LigBCon4, LigBCen7′–8, LigBCen9, and LigBCen12 to identify potentially conserved acidic amino acids that may contribute to the binding of Lig proteins to HTE. Surprisingly, Asp-341 in LigBCon4 was the only acidic amino acid conserved in all four elastin-binding immunoglobulin-like domains (Asp-341 in LigBCon4, Asp-703 in LigBCen7′–8, Asp-789 in LigBCen9, and Asp-1061 in LigBCen12) (Fig. 8*A*). To determine whether this aspartate plays a role in binding to 17–27HTE, a mutant, LigBCon4D341N, was constructed. The intrinsic fluorescence spectra of LigBCon4D341N in the absence or presence of various concentrations of 17–27HTE were recorded, and our results showed the binding affinity of LigBCon4D341N and 17–27HTE was fitted by the quenching of fluorescence intensities with a K_D of 2.44 ± 0.21 μM (Fig. 8*B*). ITC was performed to measure the binding affinity of LigBCon4D341N to 17–27HTE (K_D = 2.51 ± 0.48 μM) (Fig. 8*C* and Table 3). Interestingly, the binding affinity of LigBCon4D341N to 17–27HTE was 4.6-fold lower compared with wild type LigBCon4 (K_D = 0.50 μM from ELISA, K_D = 0.49 μM from fluorescence spectroscopy, and K_D = 0.54 μM from ITC) (Figs. 5*A* and Fig. 6 and Table 3). Moreover, the far-UV CD data of LigBCon4D341N to 17–27HTE was similar to that of wild type LigBCon4. This result rules out the possibility that the reduction of binding activity of LigBCon4D341N is because of a conformation change (supplemental Fig. 2). These data indicate that Asp-341 is a pivotal residue in LigBCon4-17-27HTE binding.

DISCUSSION

The colonization of host tissues by pathogenic *Leptospira* spp. is a pivotal factor in leptospiral pathogenesis. *Leptospira* spp. express a number of MSCRAMMs on their surfaces that promote binding to host ECMs, and they likely play an important role in leptospiral pathogenesis (10–13, 18, 20–23). *Leptospira* spp. cause severe pulmonary hemorrhage with significant mortality rates in several countries (36, 37, 47, 48) and cause abortion with placentitis (38, 49, 50). The lung and placenta are elastin-rich tissues; this led us to examine the interaction of *L. interrogans* with elastin. Our results clearly show that *L. interrogans* can adhere to both immobilized elastin peptides and tropoelastin, the precursor of elastin (Fig. 1, *A* and *B*),

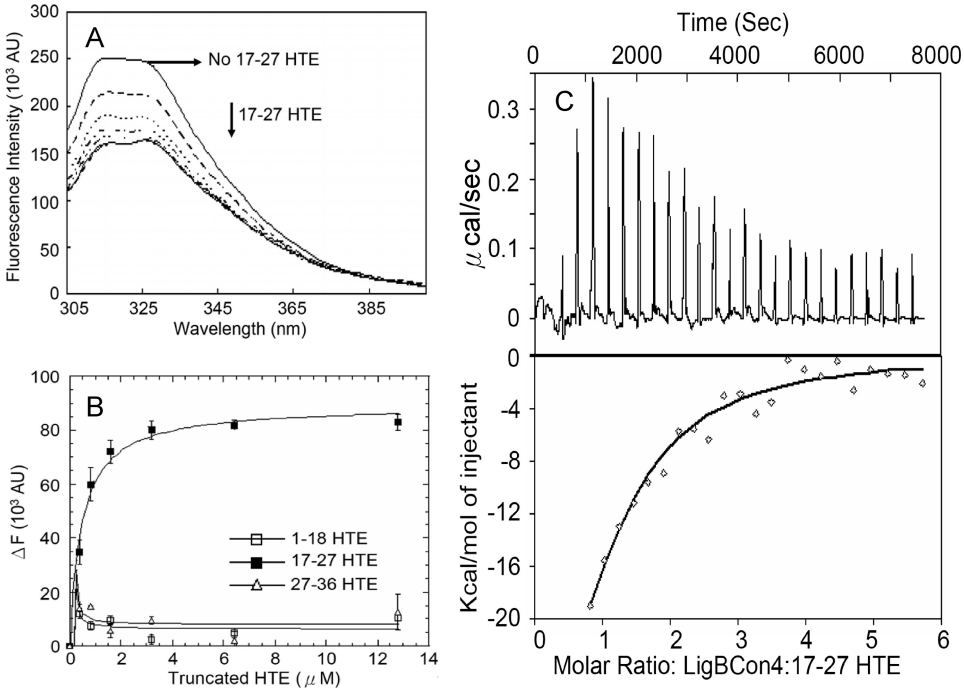

FIGURE 6. **Interaction of 17–27HTE and LigBCon4 by steady state fluorescence spectroscopy and ITC.** *A,* intrinsic fluorescence spectrum of LigBCon4 in the presence and absence of 17–27HTE. One μM of LigBCon4in Tris buffer was excited at 295 nm. Aliquots of 17–27HTE from respective stock solutions were added. The figure shows Trp fluorescence in the presence of 0, 0.4, 0.8, 1.6, 3.2, 6.4, and 12.8 μM 17–27HTE. *B,* determination of K_D value of LigBCon4 and truncated HTE by monitoring the quenching fluorescence intensities of LigBCon4 titrated by 1–18HTE, 27–36HTE (data not shown), or 17–27HTE shown in *A*. The emission wavelength recorded in this figure was 327 nm; only the titration of 17–27HTE can quench the spectrum of LigBCon4. K_D value was determined by fitting the data point into Equation 2 as described under "Materials and Methods" ($K_D = 0.49 \pm 0.07$ μM). *C,* ITC profile of LigBCon4 with 17–27HTE as a typical ITC profile in this study. *Upper panel,* heat difference obtained from 25 injections. *Lower panel,* integrated curve with experimental point (◇) and the best fit (—). The thermodynamic parameters are shown in Table 3.

and that elastin peptides extracted from tissues including lung, skin, and blood vessels can immobilize *Leptospira* as well (Fig. 1*C*). These data indicate that *L. interrogans* can bind to immobilized elastin peptides and tropoelastin.

We and others have shown that Lig proteins bind to Fn, laminin, collagen, and fibrinogen (20, 21). Therefore, we wanted to investigate whether Lig proteins can bind to elastin. Our ELISA data show that coated elastin peptides can bind to the Lig protein fragments LigBCon and LigBCen but not LigAVar or LigBCtv (Fig. 3*A*). Additionally, LigBCon and LigBCen can only partially block leptospiral binding to elastin, raising the possibility that *L. interrogans* may possess other elastin-binding proteins on its surface (Fig. 3*B*). Further studies confirming this are needed. To our surprise, LigBCon was recently shown to have no binding capacity for Fn, laminin, fibrinogen, or collagen (20, 21), but it proved capable of binding to elastin. This may explain why LigBCon is a protective antigen against *L. interrogans* serovar Pomona challenge (41). This study clearly demonstrated that Lig proteins bind to elastin, thus proving our hypothesis that one or more leptospiral MSCRAMMs bind to elastin. A recent study indicated a *ligB* mutant with an insertion containing an Spc^r cassette into the 3′ end of the *ligB* gene is still virulent in a hamster model (5). Although the reasons are unknown, there are several possibilities. 1) The truncated LigB is expressed, but at a lower level because the insertion is only in the far 3′ end of *ligB*. 2) Because the first 630 amino acids of LigA and LigB are identical, LigA may compensate for LigB in this mutant even with a similar LigA expression level. 3) LigB is not required for virulence in a hamster or rat model. 4) LigB is only needed for initial adhesion and invasion of *Leptospira* spp. moving from the environment through mucous membranes and injured skin. To answer these questions, it is essential to knock out the complete *ligA* and *ligB* genes (in-frame deletion of the complete *ligA* and *ligB* genes) and perform a virulence test using different animal models, such as dogs or monkeys.

To map the potential binding sites of Lig proteins to elastin, LigBCon and LigBCen were further truncated into several fragments, and the recombinant proteins were purified for use in an ELISA to identify the potential elastin binding domains. From our truncated constructs, we found that only LigBCon4, LigBCen7′–8, LigBCen9, and LigBCen12 can bind to elastin (Fig. 3, *D–F*). Furthermore, soluble elastin peptides can block the binding of these four truncated proteins to elastin. These data clearly indicate that there are four elastin-binding sites located on the LigB moiety (Fig. 4*A*). Although LigA and LigB contain 12 and 13 immunoglobulin-like domains, respectively, only LigBCon4, LigBCen7′–8, LigBCen9, and LigBCen12 are able to bind to elastin. This is not surprising, given that the amino acids of each immunoglobulin-like domain of LigA and LigB are so divergent (14, 16, 17).

Apart from elastin, the binding regions of LigB to HTE, the precursor of elastin, were examined by ELISA and competition binding assays, and our results indicated that the elastin binding domains of LigB, LigBCon4, LigBCen7′–8, LigBCen9, and LigBCen12 can also bind to HTE (Fig. 3*G* and Fig. 4*B*). Moreover, we demonstrated that the HTE binding region for LigBCon4, LigBCen7′–8, LigBCen9, and LigBCen12 resides in 17–27HTE, the central region of HTE (Fig. 5, *B–E*). Interestingly, FnBPA, the elastin-binding protein of *S. aureus*, was found to bind to 1–18HTE and 17–27HTE, the N-terminal region and central regions of THE, respectively (33). It suggests that binding to elastin or tropoelastin is a common mechanism for pathogen adhesion (33). However, HTE is also involved in elastogenesis, the process of elastin formation, which is pivotal for tissue repair and the regeneration of host cells. Basically, monomer HTE is expressed and excreted into the extracellular area, undergoing a rapid ordered assembly to form tropoelastin packages, a self-association process called coacervation. Lysine oxidation by lysyl oxidase facilitates cross-linking and then

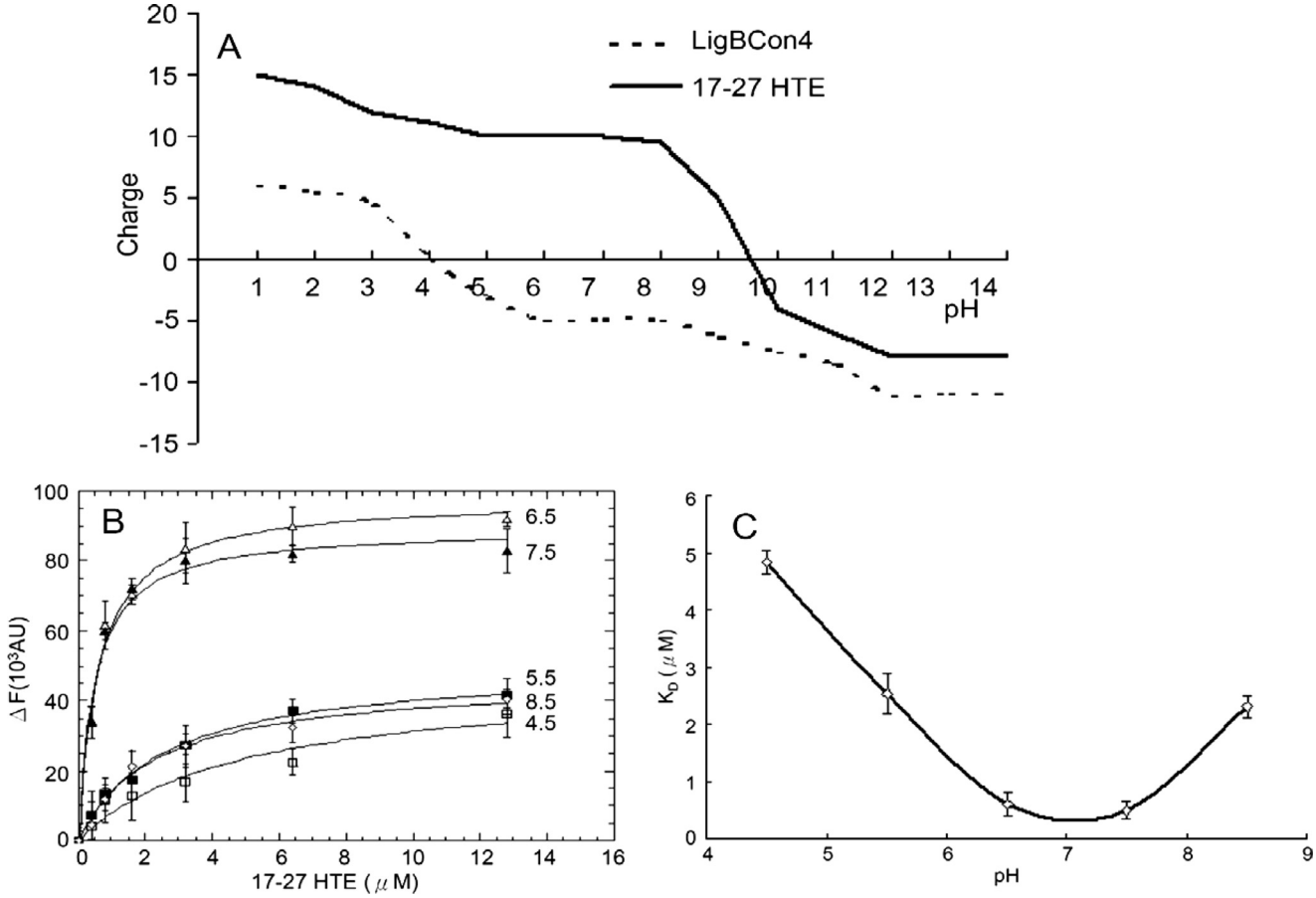

FIGURE 7. **Effect of different pH values on the binding of LigBCon4 to 17–27HTE.** *A,* titration curve for LigBCon4 and 17–27HTE. LigBCon4 (*broken line*) undergoes two-step charge transition at pH 4 and 11. 17–27 HTE (*solid line*) undergoes a charge transition at pH 9.5. *B,* determination of K_D value of LigBCon4 and 17–27HTE by monitoring the quenching fluorescence intensities of LigBCon4 at various concentrations (0, 0.4, 0.8, 1.6, 3.2, 6.4, and 12.8 μM) of 17–27HTE in Tris buffer at different pH values (4.5, 5.5, 6.5, 7.5, and 8.5). One μM LigBCon4 in Tris buffer was excited at 295 nm, and the emission wavelength recorded in this figure was 327 nm. The K_D value was determined by fitting the data point into Equation 1 as described under "Materials and Methods." *C,* LigBCon4 binding to 17–27HTE from pH 4.5 to 8.5. A plot of K_D against pH indicates that the interaction is strongly dependent on pH.

incorporation into microfibrils to generate elastic fibers (28, 32). HTE is tethered to the cell surface and probably binds to ligands, including glycosaminoglycans, integrins, and other non-ECM molecules, by its C-terminal region 27–36HTE (43, 51). Thus, Lig protein binding to 17–27HTE may not only mediate leptospiral adhesion but may also inhibit tissue regeneration by blocking the network formation (from HTE) of elastin fibers. Moreover, failed tissue repair may further facilitate the invasion of *L. interrogans* during infection.

To gain more insight into the interaction of Lig proteins with HTE, LigBCon4 was chosen for further characterization using steady state fluorescence spectroscopy and ITC techniques (Fig. 6). The K_D values obtained from both experiments are close to each other and to our ELISA results (ELISA, K_D = 0.50 ± 0.05 μM; ITC, K_D = 0.49 ± 0.07 μM; AND fluorescence spectroscopy, K_D = 0.54 ± 0.02 μM). The spectrum of LigBCon4 possesses a doublet maximum in 315 and 326 nm similar to that of LigBCen2. LigBCen2 contains a tryptophan in an immunoglobulin-like domain; indications are that this tryptophan is buried in a highly hydrophobic core (23), but the quenching of the spectra in the presence of 17–27HTE suggest the binding site of LigBCon4 may be close to this hydrophobic core containing a tryptophan. Also, the interaction of 17–27HTE and LigBCon4 is driven by enthalpy as determined by ITC (Table 3). Because enthalpy-driven reactions are generally due to charge-charge interactions or van der Waal forces, the examination of the influences of surface charges on LigBCon4 and 17–27HTE was conducted by adjusting the environmental pH. Interestingly, the optimal binding of LigBCon4 to 17–27HTE corresponds to pH 6.5–7.5, where the charge of LigBCon4 and 17–27HTE is opposite to each other and implies that binding between the two is governed by charge-charge interaction (Fig. 7). Furthermore, the structure of LigBCon4 or 17–27HTE and the binding activities of LigBCon4-17-27HTE are properly maintained from pH 4.5 to pH 8.5 when detected by CD and fluorescence spectroscopy; this indicates that the interaction can occur in slightly basic and/or acidic environments (Fig. 7, *B* and *C,* and supplemental Fig. 1).

Leptospira spp. usually invade the host through mucous membranes or injured skin and then are distributed to different organs such as the lung, liver, kidney, or placenta through spirochetemia (1). The normal range of pH in plasma is 7.38 –7.42 and that of urine ranges from 4.5 to 8.5 (52). We conclude that the pH range from 4.5 to 8.5 allows the optimal environment for LigBCon4-17-27HTE binding, facilitating adhesion of *Leptospira* spp. to tissues in these organs.

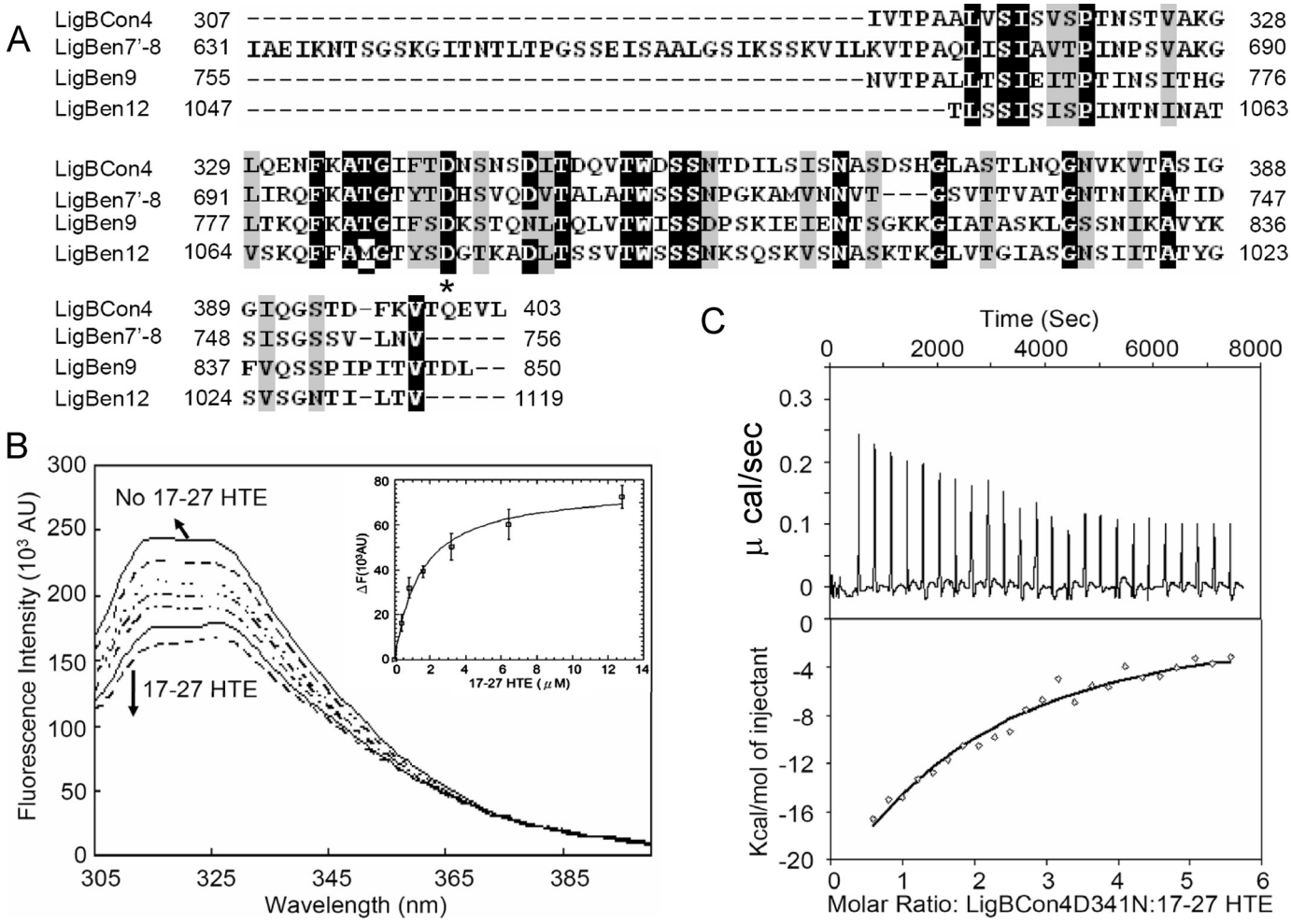

FIGURE 8. **Asp-341 is one of the important residues contributing to the LigBCon4-17-27HTE interaction.** *A,* sequence alignment of LigBCon4 (Asp-341), LigBCen7′–8 (Asp-703), LigBCen9 (Asp-789), and LigBCen12 (Asp-1061) shows that an aspartate is conserved in these four domains as indicated by an *asterisk*. The *gaps* were introduced to maximize the alignment. *Black* and *gray* colored residues indicate the conserved residues, and the homology analysis was performed with EMBL-EBI ClustalW. *B,* intrinsic fluorescence spectrum of LigBCon4D341N in the presence and absence of 17–27HTE. One μM LigBCon4D341N in Tris buffer was excited at 295 nm. Aliquots of 17–27HTE from the respective stock solutions were added. The figure shows Trp fluorescence in the presence of 0, 0.4, 0.8, 1.6, 3.2, 6.4, and 12.8 μM of 17–27HTE (*inner plot*). The determination of the K_D value of LigBCon4D35N and 17–27HTE by monitoring the quenching fluorescence intensities of LigBCon4D35N was titrated by 17–27HTE. The emission wavelength recorded in this figure was 327 nm, and K_D value was revealed by fitting the data point into Equation 2 as described under "Materials and Methods." ($K_D = 2.44 \pm 0.21$ μM). *C,* ITC profile of LigBCon4D35N with 17–27HTE as a typical ITC profile in this study. *Upper panel,* heat difference obtained from 25 injections. *Lower panel,* integrated curve with experimental point (◇) and the best fit (—). The thermodynamic parameters are shown in Table 3.

In this study, it was inferred that the interaction of LigBCon4/17–27HTE can partly be attributed to charge-charge interaction because of the enthalpy-driven interaction found by ITC (Table 3), and the acidic amino acids of LigBCon4, LigBCen7′–8, LigBCen9, and LigBCen12 participate in the binding because of the negative charge on the surface of LigBCon4 as predicted in Fig. 7*A*. The results obtained from alignment of LigBCon4, LigBCen7′–8, LigBCen9, and LigBCen12 indicate that Asp-341 of LigBCon4 is conserved in all four elastin binding immunoglobulin-like domains (Fig. 8*A*). A mutant, LigBCon4D341N, was constructed, and the binding activity of the mutated protein to 17–27HTE was analyzed by ITC and fluorescence spectroscopy to determine whether an aspartate residue is involved in the binding of LigBCon4 to 17–27HTE. The ITC and fluorescence spectroscopy results show a 4.6-fold reduction of binding activity when LigBCon4D341N was used instead of the wild type LigBCon4 (LigBCon4, $K_D = 0.54 \pm 0.02$ μM and LigBCon4D341N, $K_D = 2.51 \pm 0.48$ μM) (Fig. 8*C* and Table 3). This result further supports that the charge-charge interaction of LigBCon4 to 17–27 HTE is because of the negative charge of aspartate at physiological pH (Asp; p$K_a = 3.9$). However, the binding of 17–27HTE to LigBCon4D341N is not completely eliminated. This strongly indicates that other residues of LigBCon4 also contribute to the binding of HTE but to a lesser degree. It is not surprising that Lig proteins interact with HTE mainly through charge-charge interactions because of the biochemical nature of HTE. There are two major types of domains found in tropoelastin, including hydrophobic domains rich in nonpolar amino acids as well as hydrophilic domains rich in basic amino acids like lysine, so HTE can inherently bind to many partners via charge-charge interaction; examples include FnBPA binding to 17–27HTE and glycosaminoglycans binding to HTE (32, 53, 54).

In conclusion, we have identified that Lig proteins contribute leptospiral adhesion to elastin and HTE. Elastin and HTE binding regions on the immunoglobulin-like domains of LigBCon4,

LigBCen7′–8, LigBCen9, and LigBCen12 were mapped. Among these binding regions, LigBCon4 was found to bind to elastin and HTE with the highest affinity, and the residue Asp-341 of LigBCen4 was determined to be involved in HTE binding through charge-charge interactions. This is the first report that elastin and tropoelastin can bind to LigBCon, the conserved region of Lig from *Leptospira* spp. Further study of the interaction of Lig protein with elastin and tropoelastin is in progress in our laboratory.

Acknowledgments—We thank Drs. Timothy J. Foster, Hiroshi Wachi, and Cynthia Kinsland for kind gifts of rAFnBPA-(194–511) clone, human tropoelastin clones, and vectors (pET-THMT, pET-THGT, and pET-THST), respectively, and Dr. Marci Scidmore for kindly allowing us to use the epifluorescence microscope. We also thank Dr. Robert Oswald for the critical reading of this manuscript.

REFERENCES

1. Levett, P. N. (2001) *Clin. Microbiol. Rev.* **14,** 296–326
2. Palaniappan, R. U., Ramanujam, S., and Chang, Y. F. (2007) *Curr. Opin. Infect. Dis.* **20,** 284–292
3. Faine, S. B., Adher, B., Bolin, C., and Perolat, P. (eds) (1999) *Leptospira and Leptospirosis.,* pp. 67–69, MedSci, Medbourne, Australia
4. Verma, A., Rathinam, S. R., Priya, C. G., Muthukkaruppan, V. R., Stevenson, B., and Timoney, J. F. (2008) *Clin. Vaccine Immunol.* **15,** 1019–1023
5. Croda, J., Figueira, C. P., Wunder, E. A., Jr., Santos, C. S., Reis, M. G., Ko, A. I., and Picardeau, M. (2008) *Infect. Immun.* **76,** 5826–5833
6. Murray, G. L., Ellis, K. M., Lo, M., and Adler, B. (2008) *Microbes Infect.* **10,** 791–797
7. Murray, G. L., Srikram, A., Henry, R., Puapairoj, A., Sermswan, R., and Adler, B. (2008) *Microbes Infect.* **11,** 311–314
8. Murray, G. L., Srikram, A., Hoke, D. E., Wunder, E. A., Jr., Henry, R., Lo, M., Zhang, K., Sermswan, R. W., Ko, A. I., and Adler, B. (2008) *Infect. Immun.* **77,** 952–958
9. Patti, J. M., Allen, B. L., McGavin, M. J., and Höök, M. (1994) *Annu. Rev. Microbiol.* **48,** 585–617
10. Atzingen, M. V., Barbosa, A. S., De Brito, T., Vasconcellos, S. A., de Morais, Z. M., Lima, D. M., Abreu, P. A., and Nascimento, A. L. (2008) *BMC Microbiol.* **8,** 70
11. Barbosa, A. S., Abreu, P. A., Neves, F. O., Atzingen, M. V., Watanabe, M. M., Vieira, M. L., Morais, Z. M., Vasconcellos, S. A., and Nascimento, A. L. (2006) *Infect. Immun.* **74,** 6356–6364
12. Hauk, P., Macedo, F., Romero, E. C., Vasconcellos, S. A., de Morais, Z. M., Barbosa, A. S., and Ho, P. L. (2008) *Infect. Immun.* **76,** 2642–2650
13. Hoke, D. E., Egan, S., Cullen, P. A., and Adler, B. (2008) *Infect. Immun.* **76,** 2063–2069
14. Matsunaga, J., Barocchi, M. A., Croda, J., Young, T. A., Sanchez, Y., Siqueira, I., Bolin, C. A., Reis, M. G., Riley, L. W., Haake, D. A., and Ko, A. I. (2003) *Mol. Microbiol.* **49,** 929–945
15. Merien, F., Truccolo, J., Baranton, G., and Perolat, P. (2000) *FEMS Microbiol. Lett.* **185,** 17–22
16. Palaniappan, R. U., Chang, Y. F., Hassan, F., McDonough, S. P., Pough, M., Barr, S. C., Simpson, K. W., Mohammed, H. O., Shin, S., McDonough, P., Zuerner, R. L., Qu, J., and Roe, B. (2004) *J. Med. Microbiol.* **53,** 975–984
17. Palaniappan, R. U., Chang, Y. F., Jusuf, S. S., Artiushin, S., Timoney, J. F., McDonough, S. P., Barr, S. C., Divers, T. J., Simpson, K. W., McDonough, P. L., and Mohammed, H. O. (2002) *Infect. Immun.* **70,** 5924–5930
18. Stevenson, B., Choy, H. A., Pinne, M., Rotondi, M. L., Miller, M. C., Demoll, E., Kraiczy, P., Cooley, A. E., Creamer, T. P., Suchard, M. A., Brissette, C. A., Verma, A., and Haake, D. A. (2007) *PLoS ONE* **2,** e1188
19. Matsunaga, J., Lo, M., Bulach, D. M., Zuerner, R. L., Adler, B., and Haake, D. A. (2007) *Infect. Immun.* **75,** 2864–2874
20. Choy, H. A., Kelley, M. M., Chen, T. L., Møller, A. K., Matsunaga, J., and Haake, D. A. (2007) *Infect. Immun.* **75,** 2441–2450
21. Lin, Y. P., and Chang, Y. F. (2007) *Biochem. Biophys. Res. Commun.* **362,** 443–448
22. Lin, Y. P., and Chang, Y. F. (2008) *J. Vet. Sci.* **9,** 133–144
23. Lin, Y. P., Raman, R., Sharma, Y., and Chang, Y. F. (2008) *J. Biol. Chem.* **283,** 25140–25149
24. Faisal, S. M., Yan, W., Chen, C. S., Palaniappan, R. U., McDonough, S. P., and Chang, Y. F. (2008) *Vaccine* **26,** 277–287
25. Faisal, S. M., Yan, W., McDonough, S. P., and Chang, Y. F. (2009) *Vaccine* **27,** 378–387
26. Palaniappan, R. U., McDonough, S. P., Divers, T. J., Chen, C. S., Pan, M. J., Matsumoto, M., and Chang, Y. F. (2006) *Infect. Immun.* **74,** 1745–1750
27. Graf, R., Neudeck, H., Gossrau, R., and Vetter, K. (1996) *Cell Tissue Res.* **283,** 133–141
28. Mithieux, S. M., and Weiss, A. S. (2005) *Adv. Protein Chem.* **70,** 437–461
29. Starcher, B. C. (1986) *Thorax* **41,** 577–585
30. Vrhovski, B., Jensen, S., and Weiss, A. S. (1997) *Eur. J. Biochem.* **250,** 92–98
31. Vrhovski, B., and Weiss, A. S. (1998) *Eur. J. Biochem.* **258,** 1–18
32. Wise, S. G., and Weiss, A. S. (2009) *Int. J. Biochem. Cell Biol.* **41,** 494–497
33. Keane, F. M., Clarke, A. W., Foster, T. J., and Weiss, A. S. (2007) *Biochemistry* **46,** 7226–7232
34. Keane, F. M., Loughman, A., Valtulina, V., Brennan, M., Speziale, P., and Foster, T. J. (2007) *Mol. Microbiol.* **63,** 711–723
35. Roche, F. M., Downer, R., Keane, F., Speziale, P., Park, P. W., and Foster, T. J. (2004) *J. Biol. Chem.* **279,** 38433–38440
36. Dolhnikoff, M., Mauad, T., Bethlem, E. P., and Carvalho, C. R. (2007) *Curr. Opin. Pulm. Med.* **13,** 230–235
37. Seijo, A., Coto, H., San Juan, J., Videla, J., Deodato, B., Cernigoi, B., Messina, O. G., Collia, O., de Bassadoni, D., Schtirbu, R., Olenchuk, A., de Mazzonelli, G. D., and Parma, A. (2002) *Emerg. Infect. Dis.* **8,** 1004–1005
38. Donahue, J. M., and Williams, N. M. (2000) *Vet. Clin. North Am. Equine Pract.* **16,** 443–456, viii
39. Walsh, E. J., Miajlovic, H., Gorkun, O. V., and Foster, T. J. (2008) *Microbiology* **154,** 550–558
40. Wachi, H., Sato, F., Nakazawa, J., Nonaka, R., Szabo, Z., Urban, Z., Yasunaga, T., Maeda, I., Okamoto, K., Starcher, B. C., Li, D. Y., Mecham, R. P., and Seyama, Y. (2007) *Biochem. J.* **402,** 63–70
41. Yan, W., Faisal, S. M., McDonough, S. P., Divers, T. J., Barr, S. C., Chang, C. F., Pan, M. J., and Chang, Y. F. (2009) *Microbes Infect.* **11,** 230–237
42. Sandell, L. J., and Boyd, C. D. (eds) (1990) *Extracellular Matrix Genes,* 1st Ed., pp. 224–231, Academic Press Inc., San Diego
43. Rodgers, U. R., and Weiss, A. S. (2004) *Biochimie* **86,** 173–178
44. Böhm, G., Muhr, R., and Jaenicke, R. (1992) *Protein Eng.* **5,** 191–195
45. Sreerama, N., and Woody, R. W. (1994) *J. Mol. Biol.* **242,** 497–507
46. Pervushin, K., Riek, R., Wider, G., and Wüthrich, K. (1997) *Proc. Natl. Acad. Sci. U.S.A.* **94,** 12366–12371
47. Marotto, P. C., Nascimento, C. M., Eluf-Neto, J., Marotto, M. S., Andrade, L., Sztajnbok, J., and Seguro, A. C. (1999) *Clin. Infect. Dis.* **29,** 1561–1563
48. Wagenaar, J. F., de Vries, P. J., and Hartskeerl, R. A. (2004) *J. Travel Med.* **11,** 379–381
49. Hong, C. B., Donahue, J. M., Giles, R. C., Jr., Petrites-Murphy, M. B., Poonacha, K. B., Roberts, A. W., Smith, B. J., Tramontin, R. R., Tuttle, P. A., and Swerczek, T. W. (1993) *J. Vet. Diagnostic Invest.* **5,** 56–63
50. Sebastian, M., Giles, R., Roberts, J., Poonacha, K., Harrison, L., Donahue, J., and Benirschke, K. (2005) *Vet. Pathol.* **42,** 659–662
51. Broekelmann, T. J., Kozel, B. A., Ishibashi, H., Werneck, C. C., Keeley, F. W., Zhang, L., and Mecham, R. P. (2005) *J. Biol. Chem.* **280,** 40939–40947
52. Silverthorn, D. U. (ed) (2001) *Human Physiology, an Integrated Approach,* 2nd Ed., p. 590, Prentice-Hall, Englewood Cliffs, NJ
53. Piontkivska, H., Zhang, Y., Green, E. D., and Elnitski, L. (2004) *BMC Genomics* **5,** 31
54. Wu, W. J., Vrhovski, B., and Weiss, A. S. (1999) *J. Biol. Chem.* **274,** 21719–21724